An analysis of the FrequencyHough method for an all-sky search for continuous gravitational waves

Andrew Miller
Università di Roma: Sapienza and
The College of New Jersey

Mentor: Pia Astone
Università di Roma: Sapienza
(Dated: August 12, 2014)

In this paper we present an analysis of the Rome group's pipeline for their all-sky search for continuous gravitational waves (CW) emitted by asymmetrically rotating neutron stars. We determine how good their pipeline is at recovering CW signals that have been injected into real LIGO data (the S6 run from Hanford), in what is known as the mock data challenge (MDC). The Rome group has never worked with LIGO data before, so we also characterize the noise levels in the LIGO data and determine which parts of the frequency band have severe glitches that could inhibit future searches. Moreover we provide modifications to the pipeline that allow for future analyses for different MDCs, different stages of the pipeline and for different ways of quantifying error in the parameters of the CW signals recovered by the pipeline.

I. INTRODUCTION

Einstein's field equations imply the existence of gravitational waves. Gravitational waves propagate at the speed of light through space-time and result from massive objects moving in a nonuniform way. However they have escaped detection for almost 80 years, due to their incredibly small amplitude (on the order of 10^{-20}) relative to electromagnetic waves. Small amplitudes mean that the detection of gravitational waves is marred by seismic noise, thermal noise, shot noise, and other types of noise. This noise is only significant because the amplitudes of noise are on par with and currently greater than the amplitudes of incoming gravitational waves. That is why LIGO and VIRGO need to reduce this noise as much as possible in order to obtain the greatest probability of detection. However the data analysis techniques that will be able to confirm the detection of gravitational waves are of equal importance.

Algorithms have been developed to search for four potential sources of gravitational waves in the data. One source is from a burst, which refers to a cosmological event such as a supernova that emits strong gravitational waves for a short period of time. A second source is from compact binaries coalescing (CBC), meaning gravitational waves resulting from collisions between two neutrons stars, two black holes or a neutron star and black hole. CBCs also emit relatively strong gravitational waves for a short amount of time. A third source is from the stochastic gravitational wave background (similar to the cosmic microwave background), which are waves from early universe. These waves are much weaker than waves from bursts but are in theory always present. The last source is from an object that emits CW, which are waves that are emitted for long times on cosmological scales and change very slowly over time. However, if the observation time is long and the spin-down is large (on the order of 10^{-10} Hz/s), we will see somewhat significant changes in frequency over time.

We are using the Rome group's algorithms to search for gravitational waves emitted by asymmetrically rotating neutron stars. What this means is that there exist "bumps" on the surfaces of neutron stars (similar to mountains on earth) that in principle emit gravitational waves as neutron stars rotate. The existence of these bumps means that the rotation of the neutron star about its central axis is not perfectly symmetric. Mathematically the neutron star experiences a quadrapole moment because of this nonspherical rotation, which is responsible for the gravitational waves emission. These bumps on neutron stars are any kind of crustal deformation, which could be caused by changes in the neutron star's magnetic field or a starquake[1]. Additionally the gravitational waves from these neutron stars carry away energy, which comes from the rotational kinetic energy of the stars. As waves are emitted, the neutron stars' rates of rotation decrease over time, which is termed "spin-down." Spin-down is generally on the order of 10^{-13} Hz/s or lower, demonstrating that the energy lost via gravitational waves is very small. This continuous loss of energy implies that gravitational waves from these neutron stars will be emitted continuously but will be changing very slightly, meaning that the frequency and amplitude of each wave will be a little different with each emission.

There are in general three types of CW searches. One is called "targeted," in which everything is known about the source: its frequency, its position in the sky, etc. A second search type is called "directed," in which the position of the object in the sky is known but none of the other parameters are known. Generally targeted and directed searches are possible due to detections of celestial objects such as neutron stars with electromagnetic radiation, or from direct observation of these objects by astronomers. The final search type is the "all-sky" search: everything about the source is unknown. In these types

of searches, all possible combinations of parameters in the parameter space must be tried, so every combination of frequency, spin-down and sky position must be analyzed until our algorithms tell us that we have found a potential source. Hierarchical methods have been developed to deal with current computational problems inherent in all-sky searches (see sec. II).

Different searches have been conducted for each of these four sources, however each search has its benefits and drawbacks. For burst and CBC searches, the computation time is much lower than that of all sky searches because only one part of the sky is searched. Additionally one of the techniques used to identify these sources is known as "matched filters," in which one models the waveform for the expected signal and pushes that waveform through the data until a similar waveform is found (hence the name "matched filters"). This technique works in burst and CBC searches because the region in the sky to be analyzed is small since scientists know exactly where to look for the source. However matched filters cannot be applied to all-sky searches due to the amount of computational time required.

All-sky searches require a lot of computational time, which is a significant drawback. However the benefit is that we do not have to know where in the sky the source is, and that we can scan the entire sky for unknown sources.

Even though all-sky searches are the most computationally expensive, they offer the best way of probing the universe for gravitational waves. In the case of neutron stars, all-sky searches are needed because only about 2000 neutron stars out of the 10^9 predicted to exist in our galaxy have been identified (using electromagnetic radiation emissions). All-sky searches analyze every discretized point in the sky for potential gravitational wave signals, so when we use the Doppler shift to correct the frequency that we obtain at earth to the frequency at which the wave is emitted, we determine where in the sky the source is (see sec. II).

Searches for CBCs and bursts do not allow us to obtain a sweeping view of what kind of celestial objects emit gravitational waves: they limit us to sources that we already know exist. However gravitational waves could in theory provide more information about these sources. Moreover CBC and burst searches rely on the fact that the modelling of the waveforms is correct with some reasonable amount of certainty. But neutron star-black hole collisions, black hole-black-hole collisions, and supernovae are some of the most complicated events about which we know, and are therefore very difficult to model accurately. This means that when applying the matched filter technique, it is very possible that if we do not know what the waveforms are accurately, we will miss the detection of a gravitational wave. Additionally it is also possible that there exist objects in the universe that don't emit electromagnetic radiation but in theory could emit gravitational radiation. Detection of gravitational waves could allow us to view the universe in a different way, similar to how the discovery of radio waves started a new branch of astronomy.

The Rome group has developed a particularly efficient pipeline (a series of codes, each with a specific purpose, that contain the algorithms to search for gravitational waves) to look for CW emitted by asymmetrically rotating neutron stars. The core of this pipeline involves the Hough Transform (see sec. II). The pipeline linearly maps data collected in the time/frequency plane of the detector to the frequency/spin-down plane of the source, which is called the FrequencyHough $(FH)^2$. Other pipelines involving the Hough Transform have mapped the time/frequency data in the plane of the detector to the source position plane in the sky, the so-called Sky Hough, however this mapping is not linear and therefore has resulted in a greater amount of computational time relative to that of the Rome groups pipeline, since others employ overresolution factors in longitude and latitude, which adds many points to the parameter space. Additionally standard implementations of the Hough Transform are much more prone to artifacts, since some regions consistently appear to have a lot more candidates than expected. The FH uses an overresolution factor of 10 in frequency, which does not add anything to the computational load and allows less errors due to discretization in frequency. The specifics of this pipeline are discussed in section II.

Until now the Rome group has used VIRGO data in their pipeline, but they would like to test their algorithms with LIGO data. The group wants to now participate in the mock data challenge, which involves using the pipeline to locate and characterize (fake) signals from CW sources that have been injected into the LIGO data. Essentially we want to see whether the Rome groups pipeline can (1) work well with LIGO data and (2) effectively capture as many of the injected signals as possible, which will tell us how likely their pipeline is to detect real CWs in the future. The injected signals are from CWs emitted by asymmetrically rotating neutron stars with much larger amplitudes than these signals would actually have. Additionally the signals that we are searching for are referred to as not-blind injections, for we are given a list of signals with many relevant parameters (frequency, spin-down, location, etc.) that have been injected into the data. Once the group has recovered an acceptable number of injections, it can test its algorithms for the blind injections, that is, signals that have been injected about which the group does not know. Blind injections are meant to mimic analyzing LIGO data in the future, for we will not know the number or kind of signals that will have arrived at the detector.

II. HIERARCHICAL METHOD

Hierarchical methods reduce computational time in exchange for a small loss in sensitivity. The data are divided into small segments which are analyzed coherently,

then combined incoherently. "Coherent" analysis refers to performing fast Fourier transforms (FFTs) on individual data segments and retaining the signal's phase information: the angle at its origin and fraction of cycles that have elapsed relative to its origin. FFTs transform data taken in time to the frequency plane of the detector, so that a periodic signal would show up as a spike in the frequency plane. Once the data are combined incoherently via the FH, the phase information is lost. We are okay with losing this information since a completely coherent analysis of the data would be computationally expensive. Also it would difficult to deal with the unpredictable variations of the signal's phase during observation time.

The Rome's hierarchical method is shown in figure 1. First, we create a short FFT database (SFDB), which stores information about all of the FFTs done on segments of the data. The SFDB contains a set of windowed and interlaced FFTs for the entire frequency range of the LIGO or VIRGO detectors, such that the power of a potential CW signal later adjusted by the Doppler shift will remain within one frequency bin. Windowing and interlaced FFTs refer to performing multiple FFTs over portions of the same time in order to reduce the computational problems resulting from the truncation of an infinite time series.

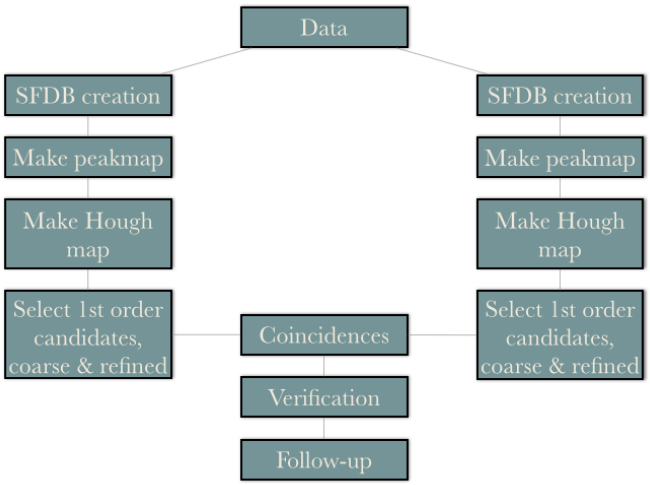

FIG. 1. Scheme of the Rome group's hierarchical method.

The width of a frequency bin is calculated as follows:

$$\delta f = \frac{1}{T_{FFT}} \tag{1}$$

T_{FFT} is the length of one FFT, which for us was 1024 seconds. We chose this length for the FFT because we are analyzing the pipeline's effectiveness for a range of frequencies in which the maximum frequency is high. The Doppler shift is directly proportional to the maximum frequency, as seen by this equation:

$$f(t) = f_0(t)\left(1 + \frac{\vec{v}\cdot\hat{n}}{c}\right) \tag{2}$$

$\vec{v}$ is the velocity of the detector relative to the solar system's center of mass, $\hat{n}$ is the vector describing the source's position in the sky, c is the speed of light, $f_0(t)$ is the frequency emitted by the source as a function of time and $f(t)$ is the time-varying frequency received on earth.

As the maximum frequency increases, the frequency that we measure differs more and more from the source frequency. We need the spread of frequencies due to the Doppler shift to remain within one frequency bin of the emitted frequency, so we need to use shorter FFTs for larger maximum frequencies (see equation 1).

Additionally for each FFT in the SFDB, we estimate the average noise of the detector across all frequencies, called the auto-regressive (AR) spectrum. The construction of the AR spectrum is quite complicated, but is constructed in such a way that the estimations in noise are unaffected by peaks in frequency and can follow both slow and sudden variations in noise.

Second, we produce peakmaps (time-frequency maps) using the information stored in the SFDB and the AR spectrum. We calculate the power spectral density S_i (the periodogram) for each FFT

$$S_i = \mid FFT \mid^2 \tag{3}$$

$$FFT = \frac{A}{\sigma} \tag{4}$$

A is the amplitude of the signal and σ is the standard deviation of the noise.

Then the ratio between the power spectral density and the auto-regressive spectrum S_i^{AR} is calculated:

$$R_i(j) = \frac{S_i}{S_i^{AR}} \tag{5}$$

This ratio is computed across all frequency bins j for the ith FFT, and is usually around 1 unless a peak at some frequency in the spectrum is present (see fig. 2a for a visual representation of this). We compare the ratios to a threshold value defined based on the number of total CW candidates we want, therefore the threshold must be chosen carefully as it affects the sensitivity of the search. A particular FFT's start time i and frequency bin j constitute a peak. The amplitude of the peak does not factor into this analysis, however we only select peaks that are local maxima. Only local maxima are selected to reduce computational time and to decrease sensitivity to glitches (huge spikes in the spectra due to noise) in exchange for a small loss in sensitivity. See fig. 2b. The peakmap

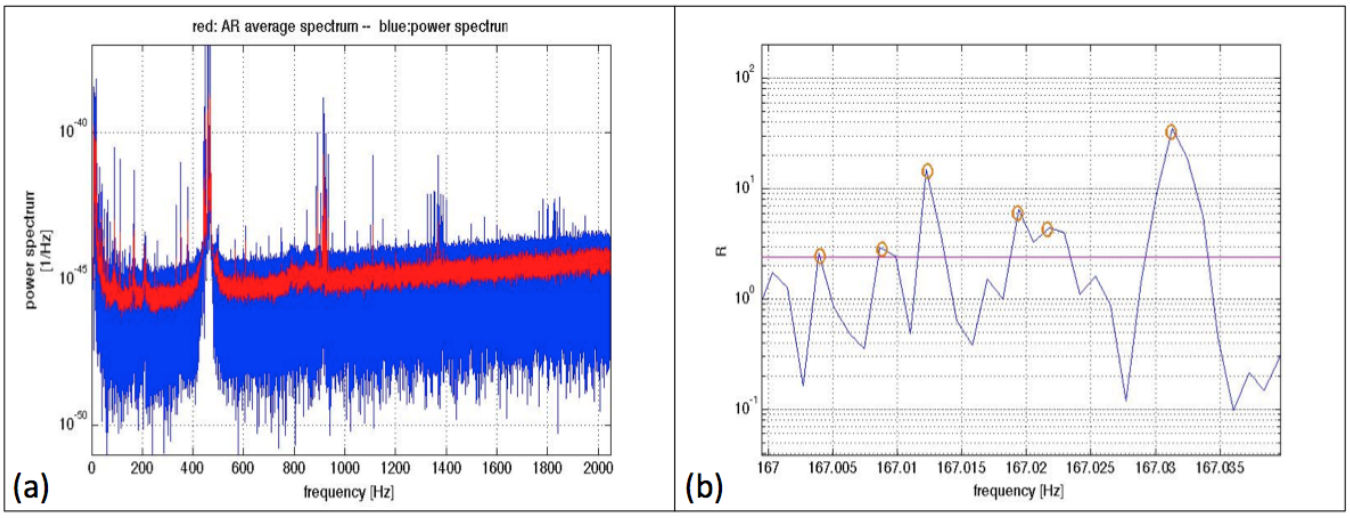

FIG. 2. (a) The auto-regressive and power spectrum are shown and (b) This is a zoomed in version of a peakmap showing the selection of just local maxima in time and frequency.

is the collection of all peaks selected. Peakmaps are the input for the FH.

Figure 3 shows zoomed in versions of a peakmap around a signal with $f = 355.725$ Hz and $\dot{f} = -2.69 \times 10^{-18}$ Hz/s before and after Doppler correction. We see that the signal is sinusoidal in nature in the non-Doppler shifted peakmap and is therefore transformed to approximately horizontal lines in the Doppler-corrected peakmap, meaning that we have effectively confined the power of this signal to less than one frequency bin. We see that this signal is particularly strong.

A. The Frequency Hough transform

The FH is a method that maps data taken in the time-frequency plane of the detector to the frequency/spin-down plane of the source in a linear manner. The method corrects for the Doppler shift, and accounts for the slowing rotation of the neutron star with the following equation:

$$f = f_0 + \dot{f}(t - t_0) + \frac{\ddot{f}}{2}(t - t_0)^2 \tag{6}$$

t_0 is the time at which the source frequency f_0 is emitted, t is the time at which we observe the (Doppler corrected) frequency f on earth, $\dot{f}$ is the source's first spin-down parameter (Hz/s) and $\ddot{f}$ is the source's second spin-down parameter, that is, how quickly in time the spin-down is changing (Hz/s/s). For the analysis conducted herein, we did not use the second spin-down parameter due to the computational load it would impose on the analysis.

Without the second spin-down parameter, this equation implies that each peak $(t-t_0,f)$ in the peakmap will be transformed into a line in the frequency/spin down plane $(f_0,\dot{f})$:

$$\dot{f} = -\frac{f_0}{(t - t_0)} + \frac{f}{(t - t_0)} \tag{7}$$

The slope of this line is $-1/(t - t_0)$. t_0 is a reference time, and it has been shown that putting this time in the middle of observation time as opposed to at the beginning or end of observation time yields better results, meaning more concentrated signals and less disturbances of nearby frequency bins. This result is due to the fact that when t_0 is at the middle of observation time, the slopes are closer to 0, which means that there is less of a disturbance of nearby frequency bins. If t_0 is at the beginning or end of observation time, all the slopes are positive or negative, respectively, which definitely contaminates nearby bins.

A CW signal in the non-Doppler shifted peakmap $(t - t_0)$ will appear as changing over time (see fig. 3), since the observed frequency of the signal is affected by the earth's rotation and the position of the source in the sky. When the frequency of the signal has been Doppler shifted, the signal will appear as a horizontal line or very close to a horizontal line if the spin-down is large (around 10^{-10} Hz/s) in the Doppler shifted peakmap $(t - t_0,f)$. The Rome group's algorithms operate well on potential CW signals, since a CW signal will in theory be mapped to around one frequency bin in the Doppler-shifted peakmap, due to the fact that we know what the waveform of a signal received at earth will look like and we can match the signal's waveform to the Doppler waveform. This means that many FFTs will capture the signal as being present. Moreover noise has an irregular form on the non-Doppler shifted peakmap, and is therefore transformed into a sinusoidal shape spread across many frequency bins. Thus not many FFTs will capture

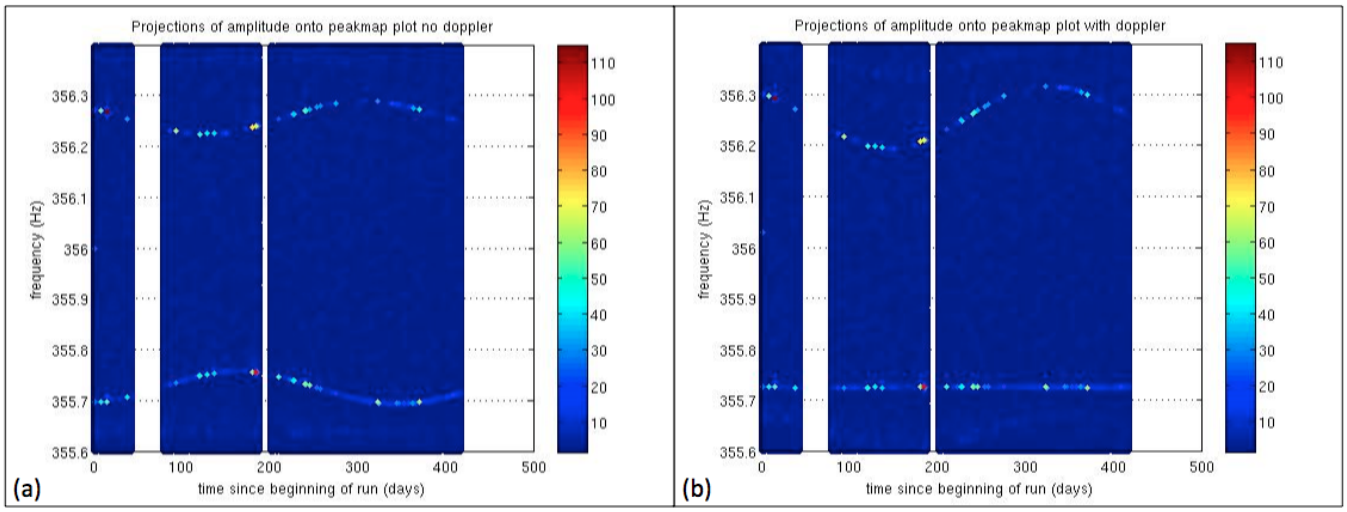

FIG. 3. (a) Pre-Doppler corrected peakmap for a signal at $f = 355.725$ Hz. The signal is visible at a sinusoidal curve, and a glitch is present at a higher frequency. (b) Doppler corrected peakmap. Signal is visible as horizontal line, glitch has had its power spread in multiple frequency bins.

the noise, unless there is a particularly strong glitch in frequency near the source's frequency.

The FH is done for every position in the sky, that is, Hough maps of the frequency/spin-down plane are constructed for each position in the sky, with the number of FFTs that captured a particular peak in the Doppler shifted peakmap $(t - t_0, f)$ colored on the map. See fig. 4 for an example of a Hough map.

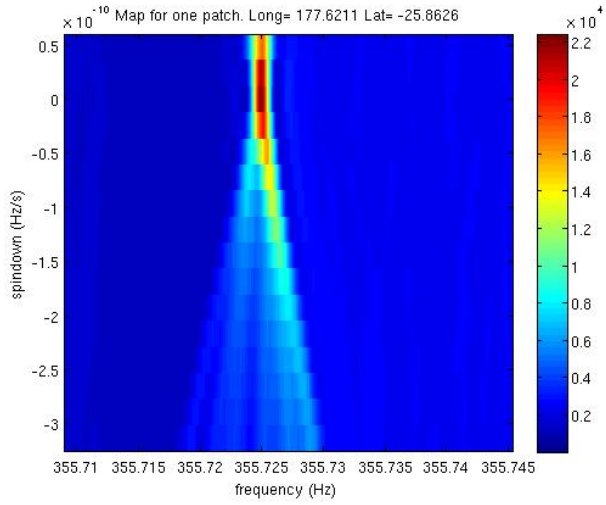

FIG. 4. This is a zoomed in version of a Hough map created for a signal at $f = 355.725Hz$, $\dot{f} = -2.69 \times 10^{-18}$, lon $= 178.0718°$, and lat $= -26.1775°$. The color bar represents the number of FFTs that captured a peak at a particular frequency/spin-down.

There are other steps that follow the FH to reduce the false alarm probability (the probability of mistakenly detecting a signal). One such step is grid refinement, in which the FH is run again around a potential CW source using a higher resolution grid. Then an analysis of coincidences is conducted, in which data from a different detector (or even data from the same detector over different times) are analyzed in search of the same signal to see if analyses of both data sets are able to recover a CW signal. There is potentially some difference in the frequency, spin-down, longitude or latitude of a signal recovered from different data sets, so we would be okay with finding a signal in a different data set within a few bins for each parameter.

However, the maximum sensitivity for the search is determined when the first candidates are selected, that is, refinement, coincidence analyses and other subsequent verification steps to reduce false alarm probability do not add any sensitivity to the search. If we miss a signal after this stage in the pipeline, we cannot recover it.

The analysis we have conducted on the efficiency of the Rome group's pipeline has focused on whether the pipeline can recover CW signals after the first FH. A coarse grid was used for the search (no refinement). A nonadaptive search was conducted, which means that we did not account for the detector's time-varying radiation pattern: we did not consider the detector's position relative to the source (whether the detector is facing the source or somewhere else). Additionally the adaptive search weights each FFT differently based on glitches that we know exist, such as the vibrational modes of the mirrors in LIGO, or parts of the data that we know are particularly disturbed. The Rome group has performed this weighting for VIRGO data, however it has not developed a weighting scheme for LIGO yet.

The Rome group also has cleaning algorithms that remove large glitches from the data, however we did not use data that had been fully cleaned. Since the Rome group has never used LIGO data before, we wanted to mini-

mize the number of variables responsible for whether the pipeline could detect fake signals injected into the data. The group wants to know in the rawest sense how good its algorithms are before trying to improve the results. The group's cleaning procedures involve removing wandering lines in frequency, which are glitches that occur somewhat regularly at different frequencies at different times. For example, wandering lines appear in Louisiana's data, when people cut down trees during a certain portion of the year, which is recorded by the LIGO as a glitch. Additionally the group performs what are known as persistency vetoes, in which they remove the known lines in frequency of the apparatus (such as the vibrational modes of the mirrors). To do persistency vetoes, the group does a histogram of the peakmap, recording the number of instances that each bin contained a peak. Bins that have an abnormally high number count are removed. The data that we used had been cleaned to the extent that some glitches in time/frequency plane were removed, but the cleaning algorithms described above were not applied.

B. Methods for the mock data challenge

We wanted to ensure that we picked a frequency band with a low amount of noise relative to other frequency bands in order to have the greatest chance of identifying the signals. We selected these bands by analyzing the glitches (spikes in the noise) in LIGO data across the 0-2000 Hz spectrum. We obtained information about these glitches in both the time and frequency domains from what are called log files. We refer to events that occur in the time domain as time events, and events that occur in the frequency domain as frequency events. In the time domain, "time" refers to when the glitch occurred in the run. In the frequency domain, "time" refers to the initial time of an FFT.

We initially conducted a search for the injected CW signals in a particular bandwidth. We modified the codes to work with any number of injected signals over the 0-2000 Hz range, so the codes will be useful when the group wants to characterize the efficiency of their algorithms for the entire bandwidth. We read in a list of these signals, and for each signal, we performed the FH on the points in the sky around the signal to determine whether the codes could accurately determine the location and frequency of the injected signal. We used the injected signals as a basis for our search because a true all-sky search requires vast amounts of computational time. A traditional all-sky search would have taken a few weeks.

Additionally in order to limit computation time and increase the probability of detecting signals, we wrote codes to search for injected signals in order of decreasing amplitude, and added functionality to the code to select as many signals to analyze as a user would like. So the user does not have to analyze every signal in a particular band, but only the top n signals.

The FH would produce many maps surrounding a particular injected signal, so we limited the number of maps based on their corresponding location in the sky relative to the injected source's location. That is, we considered maps whose corresponding locations were within a few degrees of ecliptic longitude and latitude of the injected source. The allowable error in longitude and latitude was constructed for each map based on the injected source's location. We can see this illustrated in fig. 5, which is a skymap surrounding a particular injected signal. When skymaps and Hough maps are created with the Rome group's code, higher resolution in longitude and latitude are required for higher frequencies, since the number of possible candidates increases with the square of the frequency. This means that each location in the sky will have a different amount of acceptable error in longitude and latitude, which for us is determined by the spacing between points in the skymap (see fig. 5). In practice we used half of the spacing between these points on the skymap as our error margins to select which maps to analyze. These error margins in longitude and latitude were adjusted if no maps fell within a degree of the injected source's longitude and latitude.

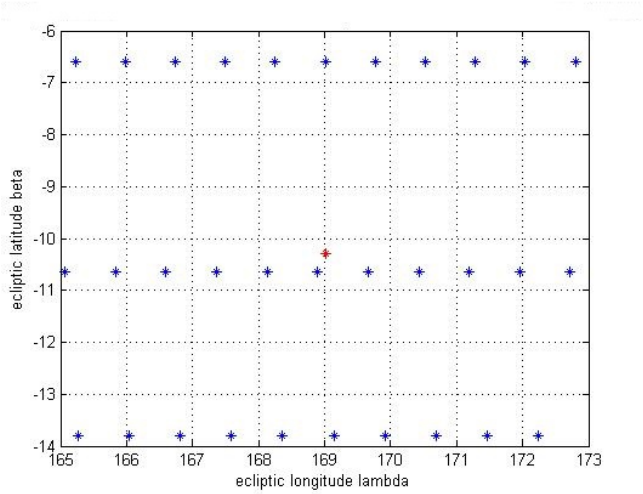

FIG. 5. A skymap created for the strongest injection in LIGO data, at f=344.735 Hz, illustrating the resolution in longitude and latitude. Thresholds were determined to be half the distance between points in longitude and latitude.

Many times, multiple Hough maps were created around a particular injection whose longitude and latitude were sufficiently close to the actual injection. In those cases, we picked the map that contained the greatest spike, that is, the map with the greatest number of FFTs corresponding to a particular frequency and spin-down. Once we selected a map with a particular longitude and latitude, we picked the frequency, spin-down and number of FFTs of the greatest spike in that particular Hough map.

To determine whether the algorithms would have found the signal, we focused on errors between the injected signal's parameters and the candidate's parameters. We analyzed differences in frequency, spin-down, longitude,

latitude and number of FFTs.

Due to the Doppler effect, the frequency of an emitted continuous gravitational wave will not be the same frequency that is observed on earth. When we take the Doppler shift into account in the FH, we know that practically there will be some error associated with the change in frequency. We quantify that error as follows: we would be able to detect a gravitational wave if its frequency lies within one frequency bin of the injected source's frequency. If the frequency of the strongest candidate in a particular Hough map was ± δf of the injected source's frequency, we would say that this source could be detected in frequency.

In many cases, the detected source's frequency was not close enough to the injected source's frequency. If this occurred, we selected 10 points on the Hough map that represented the top 10 number of peaks and their corresponding frequencies and spin-downs (that were above a certain threshold that we calculated), and determined whether the frequency closest to the injected source's frequency was within our acceptable error margins in frequency. We calculated that threshold as follows:

$$thresh = CR * \sigma + \eta \tag{8}$$

CR is the critical ratio, σ is the standard deviation of the amplitudes for a given Hough map and η is the median of the amplitudes of a given Hough map. We defined the critical ratio to be one for this analysis so that we would we select the highest peaks in a map within one standard deviation of the median. This serves to decrease the probability that a strong glitch would be responsible for a high number of peaks.

If the signal was still not found in frequency, we narrowed the frequency range around the injected signal's frequency. We selected this new frequency range based on the closest injection's frequency to the injection's frequency that we were searching for. We believe that since there are so many injections, it is possible that a stronger injection nearby the injection that we are searching for is masking the weaker injection that we are searching for. So for each injection that was not found originally, we determined how far away (in frequency) the closest injection was to the injection we were searching for, and narrowed the frequency range to ± that difference from the predicted frequency of the signal that we are looking for.

If the signal was still not found, then it was lost in frequency.

We had to also determine an acceptable error in latitude and longitude for the signals returned by the FH. We used the same margins discussed previously for ecliptic longitude and latitude, meaning that if the longitude and latitude of the signal found fell within a factor (half) of the resolution of the skymaps, then we would say that the signal could be found based on its location.

If a source's spin-down returned by the Hough fell within the resolution of spin-down values from the injected source's spin-down, that we would have found the source in spin-down. However since the pipeline is only meant at this stage to perform preliminary analyses, there is a lot of error in spin-down due to the low resolution of spin-down, which will be discussed further in section III. We calculate the resolution of the spin-down as follows:

$$\delta \dot{f} = \frac{\delta f}{T_{obs}} \tag{9}$$

$\delta \dot{f}$ is the resolution in the spin-down parameter, δ f is the width of a frequency bin and T_{obs} is the total observation time. For us, $\delta \dot{f} = 2.887 \times 10^{-10}$ Hz/s.

We conducted a similar error analysis in the number of peaks of the greatest spike in the Hough map. We computed the Hough map for the exact location in the sky of the injected source, recorded the frequency, spin-down and number of peaks of the candidate of the point on the map with the greatest number of peaks. Then we compared the number of peaks recorded by this FH to the number of peaks recorded by the FH of the nearby location in the sky. We did this comparison by setting an arbitrary number of peaks (for us it was 100) that represented the greatest possible difference between the greatest spikes in the two Hough maps created.

Figure 6 shows a schematic of the codes employed to perform this analysis. This diagram demonstrates some of the problems associated with the analysis, such as when a source's latitude did not fall into the range of input files created based on latitude, or when the threshold that was set to select the maxima on the Hough map was too high. These problems are all shown in the figure.

III. RESULTS

A. Glitch analysis to determine frequency bands

When beginning the analysis, we wanted to only search for the strongest injections in a small frequency band with a low amount of noise to maximize our chances of recovering an injection. Thus we modified the Rome group's codes for opening log files to (1) read in all of the log files for a particular run and (2) to produce a series of plots that contained information about the glitches in LIGO data for an entire run. This information is important since the Rome group has never worked with LIGO data before.

Figure 7 shows eight plots of time and frequency event glitches for the whole run, that is, glitches characterized in both the time and frequency domains.

Figure 8a and 8b show the number of glitches and strength of all glitches over the entire detection frequency band, respectively. We see that some regions are particularly disturbed, such as the 390-400 Hz frequency band. This analysis allows us to determine which bands would be good to search for injections initially.

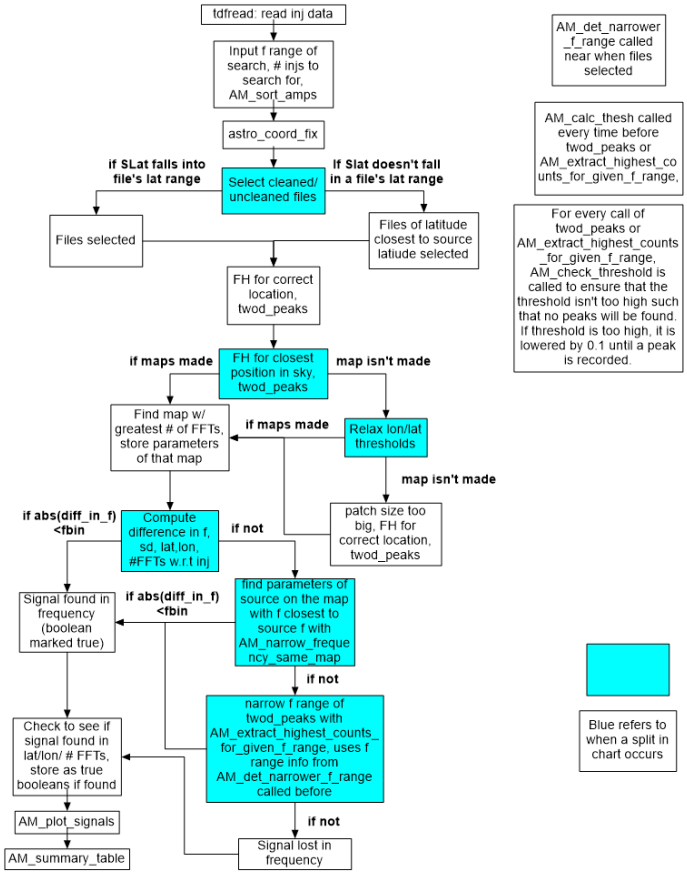

FIG. 6. Scheme of the code to search for software injections in the all-sky search

We did this analysis to characterize when glitches occurred both during the run and during the FFTs, how long the glitches were in the time and frequency planes, and the strength and glitches in time.

B. Mock data challenge

We analyzed input files that had not been cleaned and with the nonadaptive Hough initially for the 340-400 Hz band. The success of the pipeline depends heavily on the frequency band studied. In certain bands, such as between 340-350 Hz and between 390-400 Hz, we could not recover any of the injected signals initially, which amounts to 21 signals out of the 62 total signals between 340-400 Hz originally analyzed. Based on the error thresholds discussed in sec. II, we have been able to find 25% of the signals in frequency. This statistic was found before we added a method to the code to narrow the frequency range of the search if a signal was not found to account for strong injections masking the presence of weaker ones. After narrowing the frequency range, we were able to detect 35%, an improvement that will be more impactful when an analysis of the full frequency range is conducted.

Since the strongest injections were not recovered between 340-350 Hz (which are also the strongest injections in the entire spectrum), we wanted to see whether the reason that we missed these signals was due to the Rome group's algorithms or due to glitches present around that frequency. In order to answer this question, we returned to the log files and looked at the time-frequency plot created for the whole LIGO run (fig. 6b4), focusing on the strongest injection at 344.735 Hz. Figure 9 shows the projection of the number of peaks captured by the FFT onto the frequency, and we see that a "valley" exists around 344.735 Hz. It was discovered that around this frequency, the violin modes of LIGO are present, which refer to the vibrational modes of the mirrors in the detector. This particular signal was injected right around the violin mode. Since there are not many peaks recovered in that region, the background noise of other parts of the 5 Hz spectrum becomes greater than the strength of the signal, thus causing the signal to be in a valley as shown in figure 9.

We have performed an analysis of the Rome group's pipeline for the 80-700 Hz band, which contained 621 injections. In this frequency region, we have found that 31.4% (195/621) signals were within one frequency bin of injected signals. Moreover of the top 50% of injected signals in amplitude, 53.14% (165/310) of signals were found, and of the bottom 50% of injected signals in amplitude, only 9.34% (30/311) were found. This is evident from fig 10, showing a plot of injection amplitude vs frequency returned by the FH, with sources found or lost based on errors in frequency bins.

We have also created a plot (fig. 11) detailing the position in the sky where signals were found and lost. This plot allows us to see if there are particular patches in the sky where the codes recovered more signals than others. We hope to understand whether certain locations in the sky are more prone to finding or losing signals. The signals were injected into the data nonuniformly.

A summary plot (fig. 12) is shown detailing the signals that were found and lost in frequency, longitude and latitude.

It is not surprising that in all cases, a greater proportion of the top 50% of signals (recall that the signals were placed in order of decreasing amplitude) were found relative to the proportion of signals found in the bottom 50% of signals. Some plots have either the amplitude of the injected signal or the number count colored in to give a sense of the strength of the signals found and lost.

IV. DISCUSSION AND CONCLUSIONS

The Rome group's method has been evaluated at a preliminary level. Using the non-adaptive Hough and not fully cleaned data, we have established in theory the worst that the FH can be before improvements, refinements and cleaning. Unsurprisingly the group's codes are much better at detecting signals that have larger ampli-

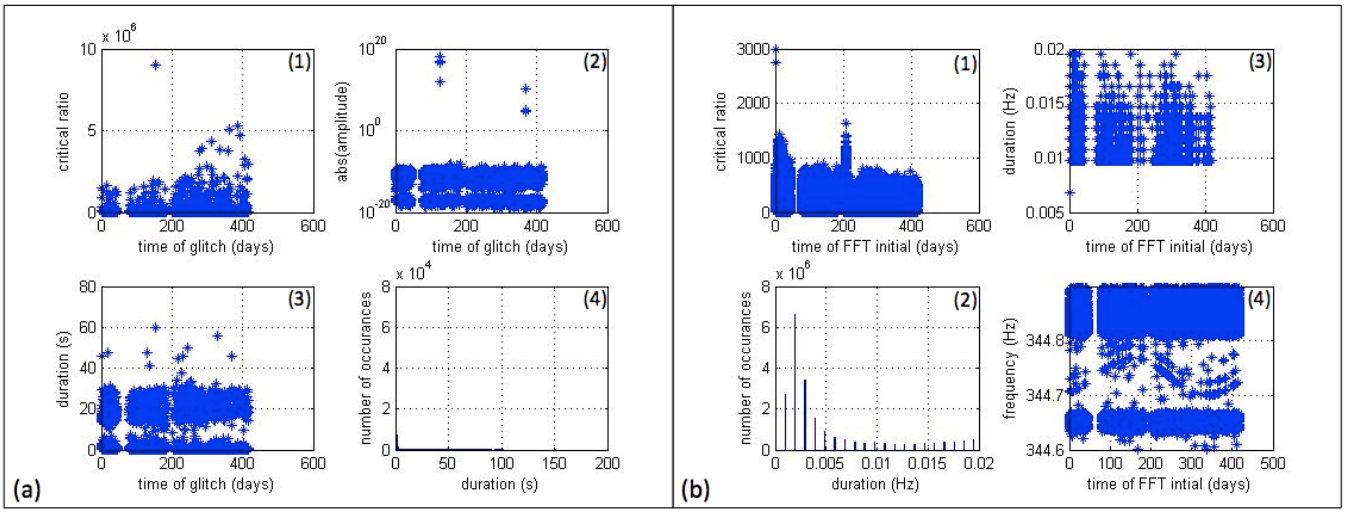

FIG. 7. (a1) Shows which periods during the run had the highest critical ratios, (a2) Shows when the strongest glitches occurred, (a3) Shows when the greatest and least number of glitches occurred, neglecting all glitches with a CR below 500, (a4) Shows the number of glitches that lasted for certain amounts of time, (b1) Shows which FFT contained each critical ratio, (b2) Shows the duration of glitches based on which FFT they occurred in, neglecting all glitches with a CR below 500 (b3) Shows the number of glitches that had particular durations, and (b4) Shows which frequencies and which FFTs gave rise to glitches, zoomed in on the strongest injection.

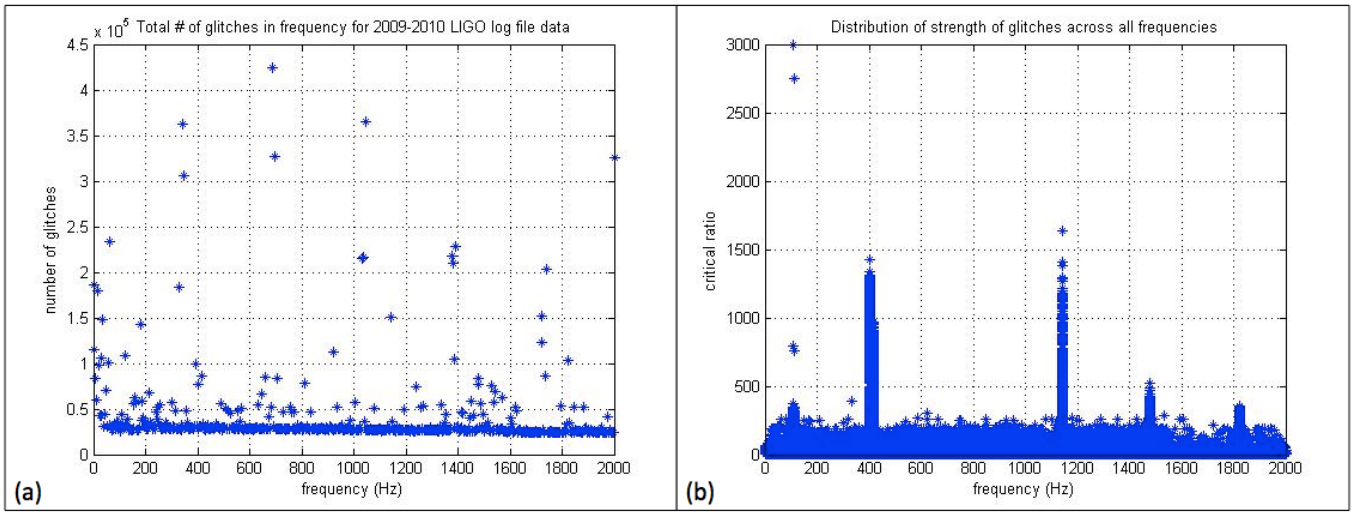

FIG. 8. (a) Distribution of the number of glitches at each frequency. Glitches have been counted and plotted every 5 Hz, (b) Strength of glitches for entire bandwidth

tudes, however further analysis must be done in order to ensure that the signals "recovered" are actually signals and not strong glitches. Moreover we must determine why each particular injection wasn't recovered: whether this was due to do large amounts of noise or due to the workings of the codes. In order to do this analysis, we must examine the amplitudes of the signals recovered to see if they are higher than the noise around them. Additionally we must do coincidence analyses, meaning that we will divide up the data into different segments to see if we detect the same CW signal in each segment. These techniques reduce the false alarm probability.

While the group's codes have done well in recovering position (based on the patch size of the Hough map), the codes have had much trouble characterizing spin-down. This is mostly due to the fact that the spin-down value for these signals is very small. The resolution of the Rome group's algorithms only 2.887×10^{-10}, however many spin-down values for injected signals are much closer to 0, on the order of 10^{-15}. This resolution of spin-down was chosen in order to limit computation time at this stage in the analysis, and can be enhanced by employing a second spin-down parameter to improve results (see equation 6).

Tables of signals found and lost were created in the

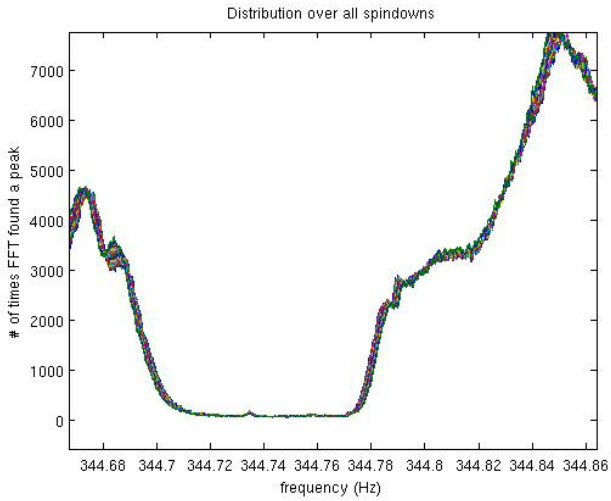

FIG. 9. Projection of number of peaks onto frequency plot showing a valley at the frequencies surrounding the strongest injection at 344.735 Hz. One can see the injection as a little bump in the valley at 344.735 Hz.

analysis, so we must now search through all of the injections that were missed to see if these injections were missed due to noise or due to the Rome group's algorithms.

This analysis was preliminary, however it focused on the most important part of the pipeline: the beginning. After the first FH transform, one either recovers or does not recover a signal. If a signal is lost at this stage, it is lost forever. The refinements are meant only to decrease the false alarm probability of signals that were detected at this stage. This stage of the pipeline is incredibly important, as it defines the maximum possible sensitivity of the pipeline for continuous gravitational wave signals.

V. ACKNOWLEDGEMENTS

We would like to thank the National Science Foundation for providing the funds for this international research experience for undergraduates. We would also like to thank Sergio Frasca, Cristiano Palomba, Sabrina D'Antonio and Matteo Digiovanni for useful discussions on the FH and other major aspects of this project. And many thanks to Pia for being an amazing adviser!

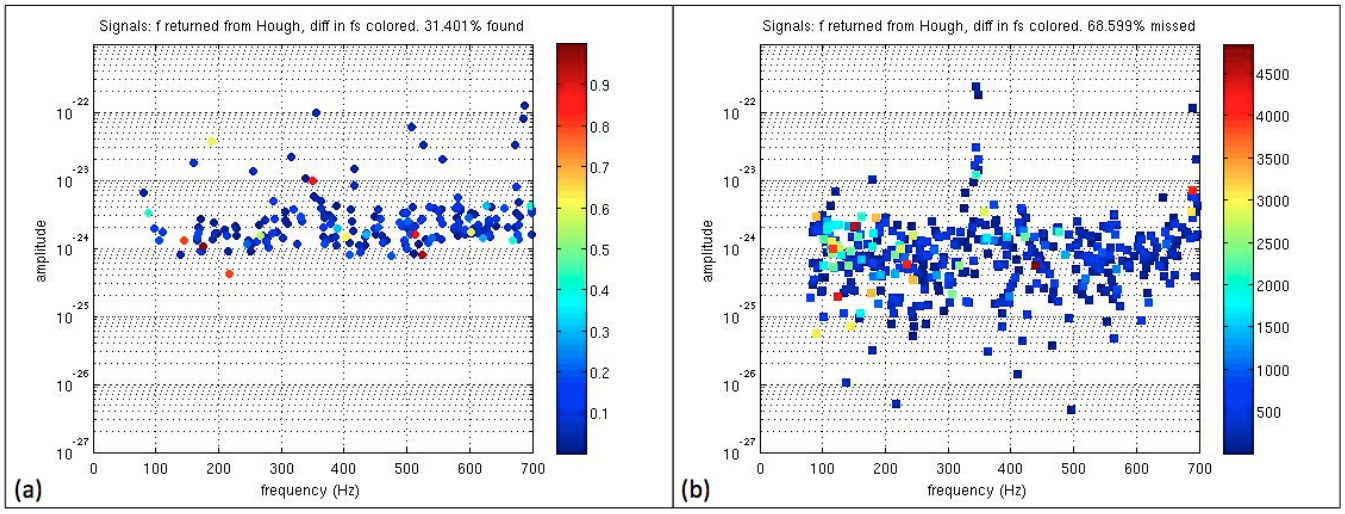

FIG. 10. Difference in number of frequency bins between injected and returned signals colored on injection amplitude vs frequency returned by FH for signals (a) found and (b) missed by the FH.

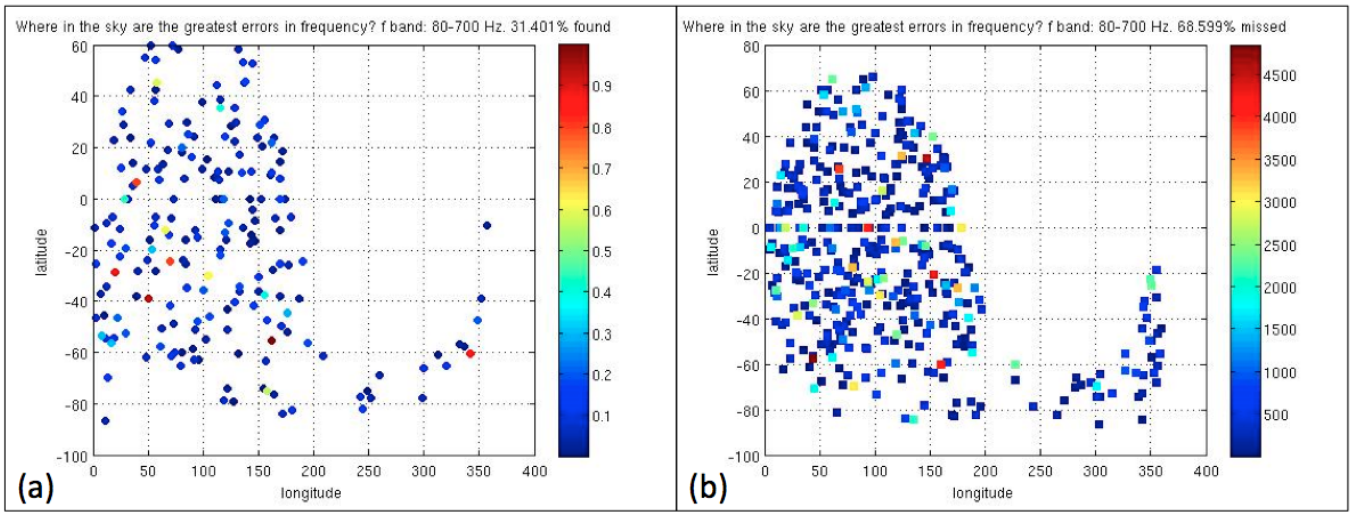

FIG. 11. Shows where in the sky signals were (a) found and (b) lost, with number of frequency bins difference between injection frequency and returned frequency colored.

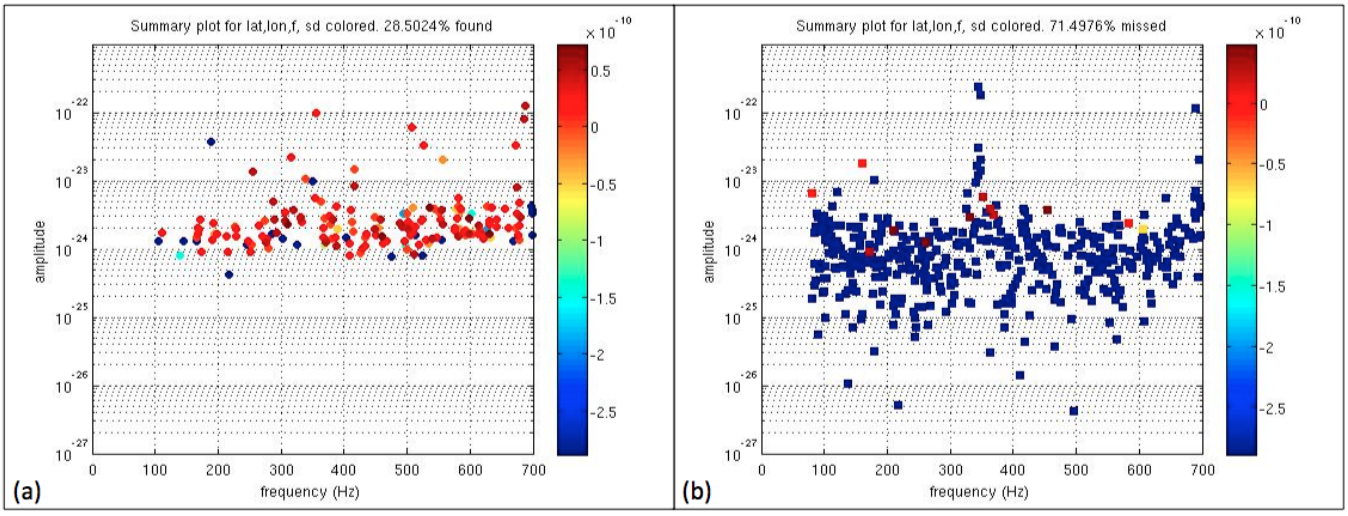

FIG. 12. Shows summary plots with spin-down returned from the FH colored for signals that, based on errors in frequency, latitude and longitude, were (a) found and (b) lost.

[1] Krishnan, B., Sintes, A. M., Papa, M. A., Schutz, B. F., Frasca, S., and Palomba, C. (2004). *Hough transform search for continuous gravitational waves.* Physical Review D, 70(8), 082001.

[2] Astone, P. et al., *A method for all-sky searches of continuous gravitational wave signals using the FrequencyHough transform.*

[3] Aasi, J., Abadie, J., Abbott, B. P., Abbott, R., Abbott, T. D., Abernathy, M., ... and Batch, J. (2013). *Prospects for localization of gravitational wave transients by the Advanced LIGO and Advanced Virgo Observatories.* arXiv preprint arXiv:1304.0670.